

2D Electronic Spectroscopy Reveals Excitonic Structure in the Baseplate of a Chlorosome

Jakub Dostál,^{†,‡} František Vácha,[§] Jakub Pšenčík,[‡] and Donatas Zigmantas*,[†]

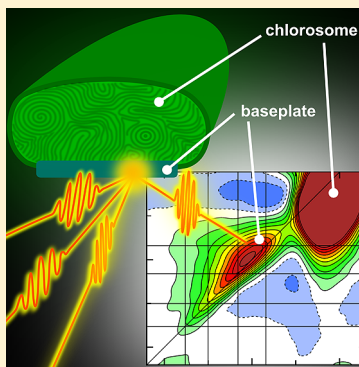
[†]Department of Chemical Physics, Lund University, P.O. Box 124, 221 00 Lund, Sweden

[‡]Faculty of Mathematics and Physics, Charles University in Prague, Ke Karlovu 3, 121 16 Prague, Czech Republic

[§]Faculty of Science, University of South Bohemia, Branišovská 31, 370 05 České Budějovice, Czech Republic

Supporting Information

ABSTRACT: In green photosynthetic bacteria, the chlorosome baseplate mediates excitation energy transfer from the interior of the light-harvesting chlorosome toward the reaction centers. However, the electronic states of the baseplate remain unexplored, hindering the mechanistic understanding of the baseplate as an excitation energy collector and mediator. Here we use two-dimensional spectroscopy to study the excited state structure and internal energy relaxation in the baseplate of green sulfur bacterium *Chlorobaculum tepidum*. We resolved an exciton system with four energy states, indicating that the organization of the pigments in the baseplate is more complex than was thought before and constitutes at least four bacteriochlorophyll molecules in a close contact. Based on the finding that the energy of the baseplate states is in the same range as in the adjacent Fenna–Matthews–Olson complex, we propose a “lateral” energy transfer pathway, where excitation energy can flow through the photosynthetic unit via all the states of individual complexes.



SECTION: Spectroscopy, Photochemistry, and Excited States

Chlorosomes serve the light-harvesting function for representatives of distinct groups of photosynthetic bacteria: green sulfur bacteria, green filamentous bacteria, and acidobacteria.^{1–4} The main structural and functional properties of the chlorosome are determined by the strong exciton interaction between a large number of self-assembled pigments. Chlorosomes typically contain $\sim 10^5$ bacteriochlorophyll (BChl) *c*, *d*, or *e* molecules coaggregated with smaller amounts of carotenoids, quinones and lipids, and it is surrounded by the lipid–protein envelope.^{1–6}

The baseplate pigment–protein complex is attached to the side of the chlorosome facing the cytoplasmic membrane and is built up from the CsmA proteins binding BChls *a*.^{1–4} The structure of the CsmA from green sulfur bacterium *Chlorobaculum (Cba.) tepidum* was determined by NMR.⁷ The CsmA proteins are arranged in a two-dimensional crystalline lattice with a spacing of 3.2–3.3 nm directly observable by electron cryomicroscopy.^{6,8} In *Cba. tepidum*, the baseplate lattice intersects the long axis of the chlorosome at an $\sim 40^\circ$ angle.⁶ However, the exact arrangement of the CsmA proteins within the baseplate, the pigment-binding geometry and stoichiometry have not yet been determined. The presence of a single conserved histidine residue in the CsmA sequence suggests there is one BChl *a* molecule per CsmA,⁹ while the experimentally obtained stoichiometry is 1–3 BChl *a* molecules per CsmA.^{10–12} Biochemical studies suggests that the baseplate building block is a CsmA dimer.¹³ Furthermore, based on the circular dichroism studies, the presence of a BChl *a* dimer in the baseplate of green sulfur bacteria was

proposed.^{14,15} Interestingly, the exciton circular dichroism signal was not observed for the isolated baseplate from green filamentous bacterium *Chloroflexus aurantiacus*.¹² A model of the baseplate based on the available information was built by Pedersen and co-workers.⁹ The energy transfer from the chlorosome to the baseplate was studied also theoretically.^{16,17} Despite all this progress, the energy structure of the baseplate is unknown.

The photosynthetic process in green sulfur bacteria begins with the capture of sunlight by the strongly absorbing BChl *c* aggregate. Initially formed delocalized excitations (excitons) randomly diffuse in the disordered chlorosome interior on the sub-100 fs time scale, as was recently observed in two-dimensional electronic spectroscopy (2DES) study.¹⁸ This process is followed by relaxation to the lower energy states of the BChl aggregates in 100–1000 fs^{19–23} before the excitation is transferred to the baseplate on a 10–100 ps time scale.^{24,25} The aggregate to baseplate transfer time depends on the species; for the BChl *c* containing green sulfur bacteria, it was determined to be 30–40 ps.^{24,26} In green sulfur bacteria and acidobacteria, the excitation energy is transferred from the baseplate putatively through the Fenna–Matthews–Olson (FMO) protein to the reaction center (RC).

Received: March 14, 2014

Accepted: April 25, 2014



In this study we used the 2DES technique to explore spectral properties of the baseplate as well as the functional connectivity between the baseplate and the low-lying exciton states of the BChl *c* aggregate. Chlorosomes were isolated from the green sulfur bacterium *Cba. tepidum* and measured at 77 K. The 2DES method utilizes the third order (in the interaction with the laser fields) response of the sample and provides simultaneously high temporal and spectral resolution that is not available in a conventional pump–probe experiment. The real part of the measured 2D spectrum can be interpreted as a collection of transient absorption spectra with an additional spectral resolution along the excitation frequency. The analysis of the obtained 2D spectra of chlorosomes provided information about the energetic structure and excitation dynamics from the low-lying states of BChl *c* aggregate to and within the baseplate. Important implications of these observations for the energy transfer from the baseplate to FMO in the intact photosystems are discussed.

The low temperature (77 K) absorption spectrum of isolated chlorosomes (Figure 1) is dominated by the BChl *c* aggregate

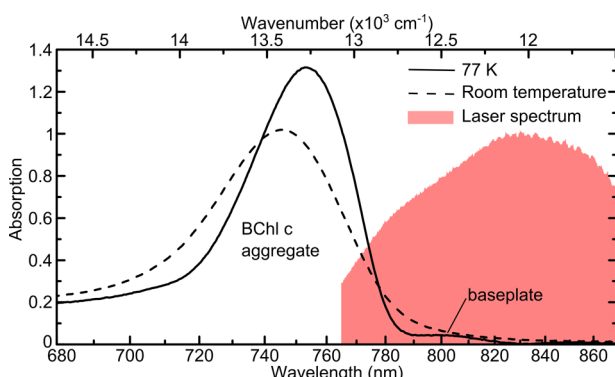


Figure 1. Absorption spectra of isolated chlorosomes from *Cba. tepidum* at room temperature (294 K) and at 77 K. The laser spectrum used in the 2DES experiments is also shown.

band peaking at 13280 cm^{-1} (753 nm). The weak, relatively broad and structureless absorption band of the baseplate complex with the maximum at 12550 cm^{-1} (797 nm) is visible in its red part. This band appears only as a shoulder of the strong aggregate band at the room temperature. In order to avoid the excessive excitation of the BChl *c* aggregate the broad laser spectrum was centered at 12050 cm^{-1} (830 nm). Hence, the blue side of the laser spectrum covered the absorption of the baseplate and only the red edge of the aggregate absorption.

Both the baseplate and aggregate are clearly visible in the acquired 2D spectra (Figure 2). At early population times (Figure 2, 30 fs spectrum) the positive baseplate signal has the shape resembling a right triangle, filling the space above the diagonal. Along the diagonal it extends between 12120 and 12700 cm^{-1} with a maximum at $\sim 12500\text{ cm}^{-1}$, which corresponds well to the absorption spectrum. The shape of the baseplate signal is determined by an overlap of the stimulated emission (SE), ground state bleach (GSB), and excited state absorption (ESA) signals. The positively signed SE from several energy states extends along the diagonal (A1–D4 in Figure 2). The GSB signal covers a corresponding square area (framed by the lines A, D, 1, and 4 in Figure 2), and is canceled by the negative ESA signal below the diagonal. Together the contributions result in a triangular-shaped positive signal with an intense diagonal part. Such signals are typical

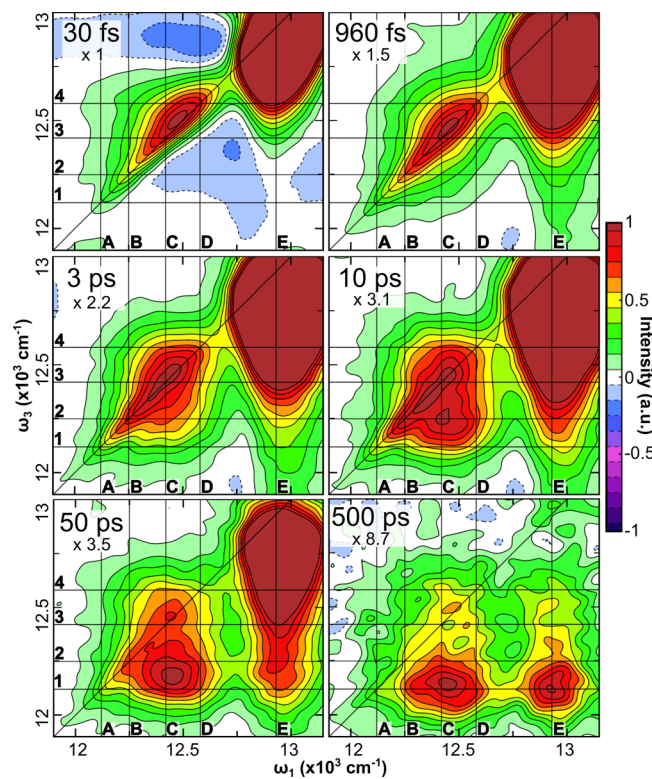


Figure 2. 2D spectra (real part) of isolated chlorosomes from *Cba. tepidum* measured at 77 K. Each frame is normalized to the baseplate maximum signal and the corresponding multiplication factor is given. Vertical and horizontal lines indicate the presumed positions of the energy states in the baseplate (D4: 12590 cm^{-1} (794 nm), C3: 12420 cm^{-1} (805 nm), B2: 12260 cm^{-1} (816 nm), A1: 12120 cm^{-1} (825 nm)). The additional vertical line E in the chlorosome region is drawn at 12940 cm^{-1} (773 nm).

signatures of excitonic systems of several coupled chromophores (see discussion below).

Due to the finite laser spectrum and limited measured detection frequency range, only the red edge of the BChl *c* aggregate peak is visible in the 2D spectra appearing at excitation frequencies higher than 12700 cm^{-1} . The peak has an asymmetric shape extending below the diagonal, which is caused by the location of the very strong peak close to the spectral detection edge and by its broad line shape. Therefore, the low energy tail that is present in the early time spectrum (Figure 2, 30 fs spectrum, positions E3 and E4) should not be interpreted as cross-peaks connecting the aggregate and baseplate transitions, which would indicate strong excitonic interaction between the two.

By following the time-evolution of the baseplate 2D spectrum, four electronic transitions were identified on the basis of the following arguments. A cross-peak C2 is clearly visible in the 10 ps 2D spectrum at an approximate (ω_1, ω_3) position of $(12420, 12260)\text{ cm}^{-1}$, indicating energy transfer between the two states at the energies marked by lines 2 and 3. Energy relaxation then continues on a longer time scale into an almost dark low-lying state located at approximately 12120 cm^{-1} . This state represents the lowest exciton state and is visible as a cross-peak (see 500 ps 2D spectrum, line 1). Lastly, upon inspection of the 30 fs 2D spectrum, it is clear that the three states identified so far are not sufficient to explain the baseplate signal, which extends to much higher energies,

indicating the presence of at least one additional energy state, tentatively located at 12590 cm^{-1} (line 4 in Figure 2).

To evaluate the energy transfer dynamics in the observed spectral region, the kinetic traces in individual points of the 2D spectrum were fitted by a sum of exponentials. Quantitative analysis of the transfer rates between the individual energy states is relatively difficult, as all points in the 2D spectrum exhibit complex multiexponential decays (see Figure S1 and S2 of the Supporting Information). However, a few salient conclusions can be made. In the baseplate part of the 2D spectra the longest time scale ($\sim 400\text{ ps}$) can be associated with the baseplate returning to the ground state. This causes a decay of the GSB contribution that extends below the entire 2D spectrum due to the excitonic interactions. The fastest processes (spanning the range of $0.3\text{--}20\text{ ps}$), on the other hand, can be connected to population relaxation between individual excitonic states of the baseplate. This transfer is reflected in the 2D spectra as redistribution of the SE signals (fading of the diagonal peaks and appearance of the cross-peaks below the diagonal), accompanied by shifting of the ESA toward higher energies. The tentative assignment of the rate constants to particular energy transfer steps is carried out by comparing the rise and decay components of the individual fits. We estimate that the first exciton relaxation step in the baseplate occurs on the time scale of a few hundred femtoseconds, the second step in a few picoseconds, and the last step in $\sim 20\text{ ps}$ (see Figure 3).

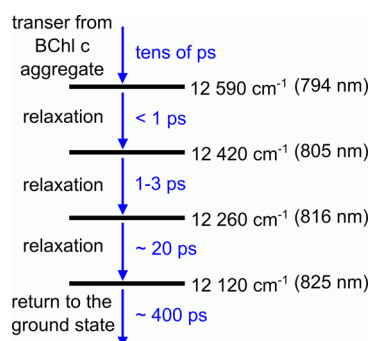


Figure 3. Proposed scheme of the exciton relaxation in the baseplate complex.

Now we examine the energy transfer from BChl *c* aggregate to the baseplate, which is clearly visible in the time-evolution of the 2D spectrum. The diagonal peak of the aggregate does not completely disappear before $\sim 200\text{ ps}$ (see Figure S1 of the Supporting Information), indicating rather slow energy transfer. This peak decays multiexponentially, which is caused by a combination of several processes: (i) exciton annihilation due to multiple photon excitations, (ii) exciton relaxation within the aggregate, and (iii) energy transfer to the baseplate. Superimposed on the population dynamics oscillatory quantum coherence dynamics (identical to the observations in ref 27) are visible during the initial 1.2 ps (see Figure S3 of the Supporting Information). Since the energy transfer from the BChl *c* aggregate to the baseplate is much slower than the relaxation within the baseplate exciton manifold, the transient populations in the higher baseplate states are rather low, as evidenced by the weak cross-peaks E2–4 (Figure 2). On the other hand, the appearance of energy transfer cross-peak at the baseplate lowest energy state (E1) is evident. All baseplate cross-peaks indicating energy flow from the aggregate to the baseplate (E1–4) exhibit

significantly longer rise times than the corresponding cross-peaks appearing after direct baseplate excitation (D1–3, C1, C2, B1) (see Figure S2 of the Supporting Information). This confirms that the BChl *c* aggregate feeds the baseplate with energy on rather long time scales, here estimated to be on the order of tens of picoseconds on the basis of time constants presented in the Figure S2 of the Supporting Information, well in the range of previously reported observations.^{24–26}

The baseplate 2D spectrum exhibits all features of a complex exciton system of at least four coupled pigments. As discussed above, the presence of four energy states of a single exciton band was identified based on their different energies and distinct dynamical properties. The most prominent feature is that all excitonic states share a common ground state and are therefore connected by an off-diagonal GSB signal. The ESA falls almost into the same region as it corresponds to transitions to the double exciton band.

We can thus deduce that at least four excitonically coupled BChl *a* molecules are in close contact within the baseplate structure. This is in contrast to previously presented models where a BChl *a* dimer was assumed.^{9,14,15} However, it is not clear whether two BChl *a* molecules are bound by a single CsmA protein, which then form a dimer as previously proposed,^{9,13} or if the proteins form a tetramer (or even more complicated structure) binding a single BChl *a* each.

The relative orientations of the four transition dipole moments of the tetramer constituents determine the distribution of oscillator strength among the individual excitonic transitions. The baseplate 2D signal is concentrated in two higher lying states (see Figure 2, 30 fs spectrum). In agreement with the exciton theory²⁸ these states exhibit the strongest ESA to the double exciton band, which explains the location of the ESA signal below the diagonal and consequently the upper-triangular shape of the 2D spectrum at early times. This indicates that the arrangement of transition dipole moments in the tetramer is closer to the H-aggregate (sandwich) than J-aggregate (head-to-tail) arrangement. However, the structure seems to be more complicated since the transition to the highest lying single exciton state would be the only allowed one, if the tetramer was an ideal H-aggregate.

It is instructive to discuss the electronic transitions (energy states) of the baseplate in a context of the light capture function of green sulfur bacteria. We find that the baseplate states are located in the same spectral region as the states of the FMO complex (Figure 4). It has been assumed that the FMO protein acts as a “molecular wire” by receiving an excitation to its high energy states localized on pigments located in a close proximity to the baseplate. Excitations then relax through the exciton

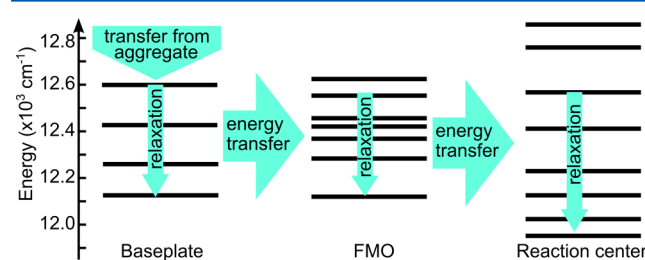


Figure 4. Proposed scheme of energy transfer within the photosynthetic apparatus of *Cba. tepidum*. The positions of energy states in FMO and RC are based on the values reported in refs 33 and 31, respectively.

manifold of FMO to the lowest state located on the other side of the complex, close to the RC, thus facilitating energy trapping by the RC.^{29,30} However, observations presented here suggest an alternative design and function of the excitation energy transfer network. We find that even the highest energy state in the baseplate is of comparable energy to the highest states in FMO, which are usually placed in the range of 12620–12890 cm⁻¹ (for a review see ref 30). A similar match is found for the lowest energy states of the baseplate and FMO (the FMO lowest state is located at 12110–12140 cm⁻¹³⁰). The energy relaxation within the baseplate observed in this study would thus be a competing process to the energy transfer directly to the highest energy states of FMO. The fraction of excitations that relax to the low-lying baseplate states in the intact photosynthetic unit depends on the energy transfer rate to FMO, which is not known. It is reasonable to expect that excitations that end up in the lower baseplate states are not lost but are “laterally” transferred into the lower FMO states (Figure 4). Interestingly, the energy states of the RC internal antenna are also located in a similar energy range as the states in FMO and the baseplate.^{31,32} Therefore, the presence of FMO does not seem to be necessary from the energetic point of view. Perhaps it has a dual function: as a spacer, which allows ferredoxin to access RCs³⁴ putatively located under the chlorosome, and at the same time, as the energy conduit, transferring excitation energy from the baseplate to the RCs. Ferredoxins are water-soluble electron acceptors employed by type I RCs, which are found in green sulfur bacteria and acidobacteria, but not by type II RCs, which might explain the absence of FMO in green filamentous bacteria.

The overall energy flow through the photosynthetic unit of green sulfur bacteria is apparently very complex and depends on the relaxation rates within subunits and of energy transfer rates between the different states in the subunits. We expect that the 2DES experiments on the intact photosynthetic units should be able to unravel the complexity of the energy collection function.

In conclusion, the energy structure of the baseplate exhibits spectroscopic features typical of an excitonic system of four coupled molecules, implying that the baseplate structure is more complex than it was believed before. After the excitation energy is transferred from the BChl *c* aggregate to the baseplate, and relaxes between the individual states with each energy transfer step occurring on a distinctive time scale. The energy of the baseplate states suggests an alternative energy flow pathway in the photosynthetic unit of green sulfur bacteria where the excitations captured by the chlorosome is transferred via all the states of the baseplate and FMO complexes to the RC.

EXPERIMENTAL METHODS

The *Chlorobaculum tepidum* cell culture was grown as described previously,³⁵ and chlorosomes were isolated and purified according to the standard procedure using two successive sucrose gradient ultracentrifugation steps.³⁶ Prior to experiments, the chlorosome solution was dissolved in 1:2 (v/v) ratio in glycerol, reduced by 20 mM sodium dithionite and incubated for 2 h in an airtight vessel. The sample optical density was approximately 0.05 in the baseplate region at 12500 cm⁻¹ in the 0.5 mm optical path demountable cell. All 2DES experiments were carried out at 77 K in an optical cryostat (Oxford Optistat DN). The energy of 17 fs long excitation pulses produced at a 20 kHz repetition rate was 1.5 nJ per pulse, and the beams were

focused to the spot size of ~100 μ m in diameter, which corresponds to a flux of $\sim 8 \times 10^{13}$ photons/pulse/cm².

The 2D spectra were obtained using a setup described in detail in the Supporting Information or in refs 37 and 38. The spectral resolution along the excitation and detection axis is about 65 and 50 cm⁻¹, respectively.

ASSOCIATED CONTENT

Supporting Information

Kinetic traces taken from distinct peaks in the 2D spectra, their multiexponential fits, and a description of the experimental setup. This material is available free of charge via the Internet at <http://pubs.acs.org>.

AUTHOR INFORMATION

Corresponding Author

*Address: Department of Chemical Physics, Lund University, P.O. Box 124, 22100 Lund, Sweden. E-mail: donatas.zigmantas@chemphys.lu.se; Phone: +46 46 2224769; Fax: +46 46 2224119.

Notes

The authors declare no competing financial interest.

ACKNOWLEDGMENTS

We would like to thank E. Thyrhaug for critically reading the manuscript. The work in Lund was supported by the Swedish Research Council and the Knut and Alice Wallenberg Foundation. The work in Prague and České Budějovice was supported by the Czech Science Foundation (Project P501/12/G055).

REFERENCES

- (1) Frigaard, N.-U.; Bryant, D. A. Chlorosomes: Antenna Organelles in Photosynthetic Green Bacteria. In *Complex Intracellular Structures in Prokaryotes*; Shively, J., Ed.; Springer: Berlin/Heidelberg, 2006; Vol. 2, pp 79–114.
- (2) Bryant, D. A.; Costas, A. M. G.; Maresca, J. A.; Chew, A. G. M.; Klatt, C. G.; Bateson, M. M.; Tallon, L. J.; Hostetler, J.; Nelson, W. C.; Heidelberg, J. F.; et al. *Candidatus Chloracidobacterium Thermophilum*: An Aerobic Phototrophic Acidobacterium. *Science* **2007**, *317*, 523–526.
- (3) Blankenship, R. E.; Matsuura, K. Antenna Complexes from Green Photosynthetic Bacteria. In *Light-Harvesting Antennas in Photosynthesis*; Green, B. R.; Parson, W. W., Eds.; Kluwer Academic Publishers: Dordrecht, The Netherlands, 2003; pp 195–217.
- (4) Blankenship, R. E.; Olson, J. M.; Miller, M. Antenna Complexes from Green Photosynthetic Bacteria. In *Anoxygenic Photosynthetic Bacteria*; Blankenship, R.; Madigan, M.; Bauer, C., Eds.; Springer: Heidelberg, The Netherlands, 1995; pp 399–435.
- (5) Orf, G. S.; Blankenship, R. E. Chlorosome Antenna Complexes from Green Photosynthetic Bacteria. *Photosynth. Res.* **2013**, *116*, 315–331.
- (6) Oostergetel, G. T.; van Amerongen, H.; Boekema, E. J. The Chlorosome: A Prototype for Efficient Light Harvesting in Photosynthesis. *Photosynth. Res.* **2010**, *104*, 245–255.
- (7) Pedersen, M. Ø.; Underhaug, J.; Dittmer, J.; Miller, M.; Nielsen, N. C. The Three-Dimensional Structure of CsmA: A Small Antenna Protein from the Green Sulfur Bacterium *Chlorobium Tepidum*. *FEBS Lett.* **2008**, *582*, 2869–2874.
- (8) Pšenčík, J.; Collins, A. M.; Liljeroos, L.; Torkkeli, M.; Laurinmäki, P.; Ansink, H. M.; Ikonen, T. P.; Serimaa, R. E.; Blankenship, R. E.; Tuma, R.; et al. Structure of Chlorosomes from the Green Filamentous Bacterium *Chloroflexus Aurantiacus*. *J. Bacteriol.* **2009**, *191*, 6701–6708.

(9) Pedersen, M. Ø.; Linnanto, J.; Frigaard, N.-U.; Nielsen, N. C.; Miller, M. A Model of the Protein–Pigment Baseplate Complex in Chlorosomes of Photosynthetic Green Bacteria. *Photosynth. Res.* **2010**, *104*, 233–243.

(10) Bryant, D. A.; Vassilieva, E. V.; Frigaard, N.; Li, H. Selective Protein Extraction from *Chlorobium Tepidum* Chlorosomes Using Detergents. Evidence That CsmA Forms Multimers and Binds Bacteriochlorophyll a. *Biochemistry* **2002**, *41*, 14403–14411.

(11) Sakuragi, Y.; Frigaard, N.; Shimada, K.; Matsuura, K. Association of Bacteriochlorophyll a with the CsmA Protein in Chlorosomes of the Photosynthetic Green Filamentous Bacterium *Chloroflexus Aurantiacus*. *Biochim. Biophys. Acta* **1999**, *1413*, 172–180.

(12) Montaño, G. A.; Wu, H.-M.; Lin, S.; Brune, D. C.; Blankenship, R. E. Isolation and Characterization of the B798 Light-Harvesting Baseplate from the Chlorosomes of *Chloroflexus Aurantiacus*. *Biochemistry* **2003**, *42*, 10246–10251.

(13) Vassilieva, E. V.; Stirewalt, V. L.; Jakobs, C. U.; Frigaard, N.-U.; Inoue-Sakamoto, K.; Baker, M. A.; Sotak, A.; Bryant, D. A. Subcellular Localization of Chlorosome Proteins in *Chlorobium Tepidum* and Characterization of Three New Chlorosome Proteins: CsmF, CsmH, and CsmX. *Biochemistry* **2002**, *41*, 4358–4370.

(14) Gerola, P. D.; Olson, J. M. A New Bacteriochlorophyll a–Protein Complex Associated with Chlorosomes of Green Sulfur Bacteria. *Biochim. Biophys. Acta, Bioenerg.* **1986**, *848*, 69–76.

(15) Pedersen, M. Ø.; Pham, L.; Steensgaard, D. B.; Miller, M. A Reconstituted Light-Harvesting Complex from the Green Sulfur Bacterium *Chlorobium Tepidum* Containing CsmA and Bacteriochlorophyll a. *Biochemistry* **2008**, *47*, 1435–1441.

(16) Huh, J.; Saikin, S. K.; Brookes, J. C.; Valleau, S.; Fujita, T.; Aspuru-Guzik, A. Atomistic Study of Energy Funneling in the Light-Harvesting Complex of Green Sulfur Bacteria. *J. Am. Chem. Soc.* **2014**, *136*, 2048–2057.

(17) Linnanto, J. M.; Korppi-Tommola, J. E. I. Exciton Description of Chlorosome to Baseplate Excitation Energy Transfer in Filamentous Anoxygenic Phototrophs and Green Sulfur Bacteria. *J. Phys. Chem. B* **2013**, *117*, 11144–11161.

(18) Dostál, J.; Mančal, T.; Augulis, R.; Vácha, F.; Pšenčík, J.; Zigmantas, D. Two-Dimensional Electronic Spectroscopy Reveals Ultrafast Energy Diffusion in Chlorosomes. *J. Am. Chem. Soc.* **2012**, *134*, 11611–11617.

(19) Savikhin, S.; Zhu, Y.; Blankenship, R. E.; Struve, W. S. Intraband Energy Transfers in the BChl c Antenna of Chlorosomes from the Green Photosynthetic Bacterium *Chloroflexus Aurantiacus*. *J. Phys. Chem.* **1996**, *100*, 17978–17980.

(20) Martiskainen, J.; Linnanto, J.; Kananavičius, R.; Lehtovaara, V.; Korppi-Tommola, J. Excitation Energy Transfer in Isolated Chlorosomes from *Chloroflexus Aurantiacus*. *Chem. Phys. Lett.* **2009**, *477*, 216–220.

(21) Martiskainen, J.; Linnanto, J.; Aumanen, V.; Myllyperkiö, P.; Korppi-Tommola, J. Excitation Energy Transfer in Isolated Chlorosomes from *Chlorobaculum tepidum* and *Prosthecochloris aestuarii*. *Photochem. Photobiol.* **2012**, *88*, 675–683.

(22) Savikhin, S.; van Noort, P. I.; Zhu, Y.; Lin, S.; Blankenship, R. E.; Struve, W. S. Ultrafast Energy Transfer in Light-Harvesting Chlorosomes from the Green Sulfur Bacterium *Chlorobium Tepidum*. *Chem. Phys.* **1995**, *194*, 245–258.

(23) Pšenčík, J.; Ma, Y.-Z.; Arellano, J. B.; Hála, J.; Gillbro, T. Excitation Energy Transfer Dynamics and Excited-State Structure in Chlorosomes of *Chlorobium Phaeobacteroides*. *Biophys. J.* **2003**, *84*, 1161–1179.

(24) Causgrove, T. P.; Brune, D. C.; Blankenship, R. E. Förster Energy Transfer in Chlorosomes of Green Photosynthetic Bacteria. *J. Photochem. Photobiol. B: Biol.* **1992**, *15*, 171–179.

(25) Causgrove, T. P.; Brune, D. C.; Wang, J.; Wittmershaus, B. P.; Blankenship, R. E. Energy Transfer Kinetics in Whole Cells and Isolated Chlorosomes of Green Photosynthetic Bacteria. *Photosynth. Res.* **1990**, *26*, 39–48.

(26) Van Noort, P. I.; Zhu, Y.; LoBrutto, R.; Blankenship, R. E. Redox Effects on the Excited-State Lifetime in Chlorosomes and Bacteriochlorophyll c Oligomers. *Biophys. J.* **1997**, *72*, 316–325.

(27) Dostál, J.; Mančal, T.; Vácha, F.; Pšenčík, J.; Zigmantas, D. Unraveling the nature of coherent beatings in chlorosomes. *J. Chem. Phys.* **2014**, *140*, 115103.

(28) Van Amerongen, H.; Valkunas, L.; van Grondelle, R. *Photosynthetic Excitons*; World Scientific: Singapore, 2000.

(29) Schmidt Am Busch, M.; Müh, F.; El-Amine Madjet, M.; Renger, T. The Eighth Bacteriochlorophyll Completes the Excitation Energy Funnel in the FMO Protein. *J. Phys. Chem. Lett.* **2011**, *2*, 93–98.

(30) Milder, M. T. W.; Brüggemann, B.; van Grondelle, R.; Herek, J. L. Revisiting the Optical Properties of the FMO Protein. *Photosynth. Res.* **2010**, *104*, 257–274.

(31) Hauska, G.; Schoedl, T.; Remigy, H.; Tsiotis, G. The Reaction Center of Green Sulfur Bacteria. *Biochim. Biophys. Acta* **2001**, *1507*, 260–277.

(32) Permentier, H. P.; Schmidt, K. A.; Kobayashi, M.; Akiyama, M.; Hager-Braun, C.; Neerken, S.; Miller, M.; Amesz, J. Composition and Optical Properties of Reaction Centre Core Complexes from the Green Sulfur Bacteria *Prosthecochloris aestuarii* and *Chlorobium tepidum*. *Photosynth. Res.* **2000**, *64*, 27–39.

(33) Abramavicius, D.; Voronine, D. V.; Mukamel, S. Double-Quantum Resonances and Exciton-Scattering in Coherent 2D Spectroscopy of Photosynthetic Complexes. *Proc. Natl. Acad. Sci. U. S. A.* **2008**, *105*, 8525–8530.

(34) Wen, J. Z.; Zhang, H.; Gross, M. L.; Blankenship, R. E. Membrane orientation of the FMO antenna protein from *Chlorobaculum tepidum* as determined by mass spectrometry-based footprinting. *Proc. Natl. Acad. Sci.* **2009**, *106*, 6134–6139.

(35) Pšenčík, J.; Ikonen, T. P.; Laurinmäki, P.; Merckel, M. C.; Butcher, S. J.; Serimaa, R. E.; Tuma, R. Lamellar Organization of Pigments in Chlorosomes, the Light Harvesting Complexes of Green Photosynthetic Bacteria. *Biophys. J.* **2004**, *87*, 1165–1172.

(36) Steensgaard, D. B.; Matsuura, K.; Cox, R. P.; Miller, M. Changes in Bacteriochlorophyll c Organization during Acid Treatment of Chlorosomes from *Chlorobium tepidum*. *Photochem. Photobiol.* **1997**, *65*, 129–134.

(37) Augulis, R.; Zigmantas, D. Two-Dimensional Electronic Spectroscopy with Double Modulation Lock-in Detection: Enhancement of Sensitivity and Noise Resistance. *Opt. Express* **2011**, *19*, 13126–13133.

(38) Augulis, R.; Zigmantas, D. Detector and Dispersive Delay Calibration Issues in Broadband 2D Electronic Spectroscopy. *J. Opt. Soc. Am. B* **2013**, *30*, 1770–1774.

SUPPORTING INFORMATION

2D Electronic Spectroscopy Reveals Excitonic Structure in the Baseplate of a Chlorosome

Jakub Dostál ^{a,b}, František Vácha ^c, Jakub Pšenčík ^b, Donatas Zigmantas ^{a*}

^a Department of Chemical Physics, Lund University, P.O. Box 124, 221 00 Lund, Sweden

^b Faculty of Mathematics and Physics, Charles University in Prague, Ke Karlovu 3, 121 16 Prague, Czech Republic

^c Faculty of Science, University of South Bohemia, Branišovská 31, 370 05 České Budějovice, Czech Republic

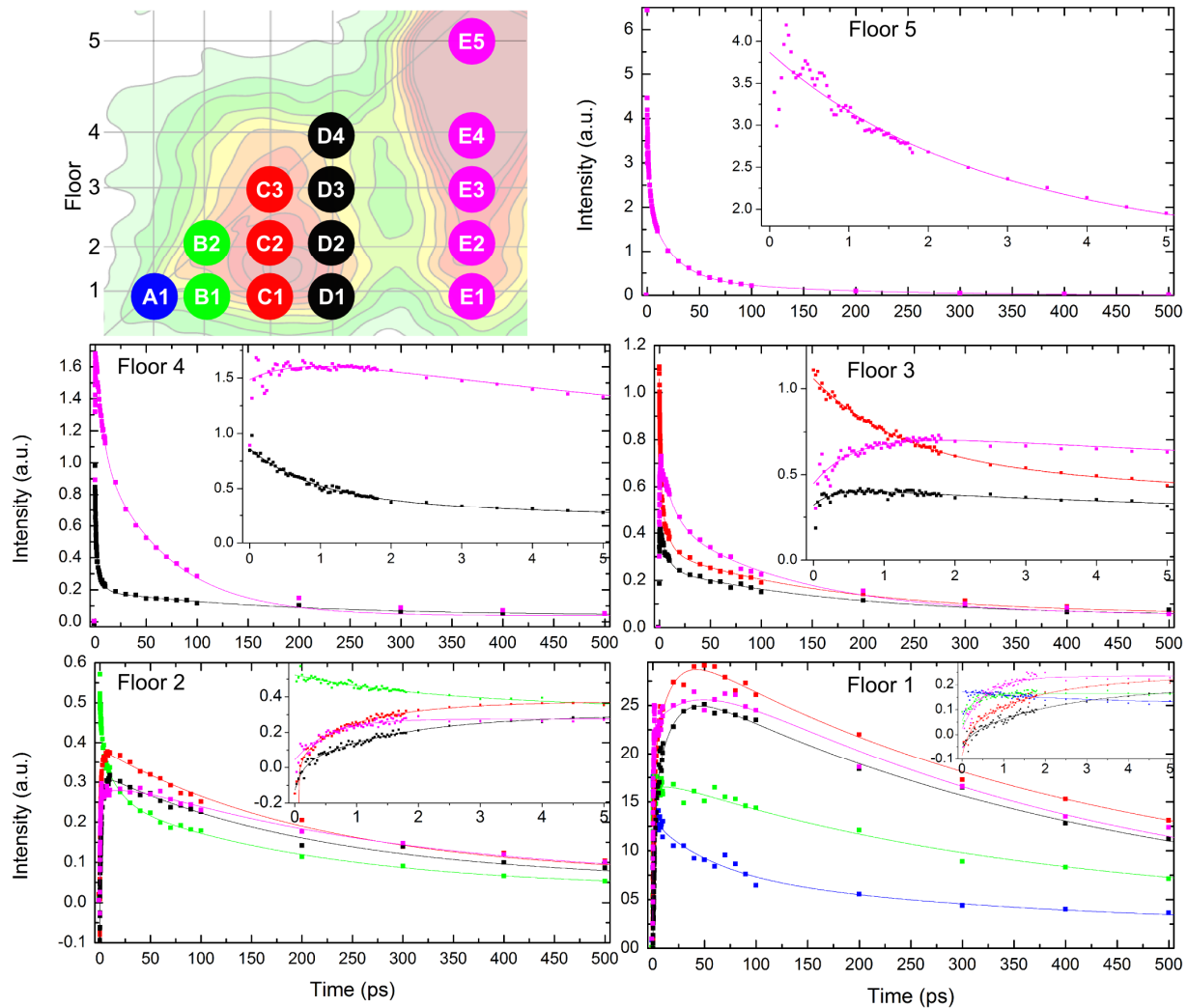


Figure S1: Time evolution of the individual points in the 2D spectrum fit by multiple decaying exponentials. Each graph contains time evolution curves of a set of distinctive peaks at the same detection frequency (ω_3) and different excitation frequency (ω_1). The color coding of curves is according to the legend in the top-left-handed corner, where each color disc corresponds to one diagonal peak or cross-peak arranged as in the experimental 2D spectrum and denoted by the gridline markers (Fig. 2).

SUPPORTING INFORMATION

		Chromosome		
		(2.3 ± 0.4) ps ↓	46% of 3.87	
		(20 ± 10) ps ↓	43%	
		(140 ± 200) ps ↓	11%	
Baseplate		(0.89 ± 0.09) ps ↓ (6 ± 1) ps ↓ (185 ± 60) ps ↓ ∞	51% of 0.86 27% 18% 4%	(0.7 ± 0.2) ps ↑ (7 ± 2) ps ↓ (67 ± 8) ps ↓ ∞
		(1.2 ± 0.1) ps ↓ (7 ± 2) ps ↓ (170 ± 30) ps ↓ ∞	44% of 1.06 25% 25% 5%	(0.26 ± 0.05) ps ↑ (7.5 ± 0.9) ps ↓ (180 ± 30) ps ↓ ∞
		(2.0 ± 0.4) ps ↓ (17 ± 7) ps ↓ (210 ± 50) ps ↓ ∞	25% of 0.52 25% 43% 7%	(0.03 ± 0.01) ps ↑ (0.4 ± 0.2) ps ↑ (1.5 ± 0.4) ps ↑ ∞
		(2.8 ± 0.8) ps ↓ (60 ± 60) ps ↓ (400 ± 800) ↓ ∞	25% of 0.17 31% 14% 11%	(0.26 ± 0.03) ps ↑ 17 ps ↑ (400 ± 100) ps ↓ ∞

Figure S2: Time constants of and relative amplitudes obtained from multiexponential fits of individual points in the 2D spectrum. Each cell contains information about the evolution of the single distinct peak in the 2D spectrum. The cells are arranged in the way the peaks appear in the 2D spectrum. The color-coding is identical as in Supplementary Fig. 1. Decaying and rising components are marked by the black and red colors, correspondingly. The total amplitude of each curve is marked at the right side of each cell.

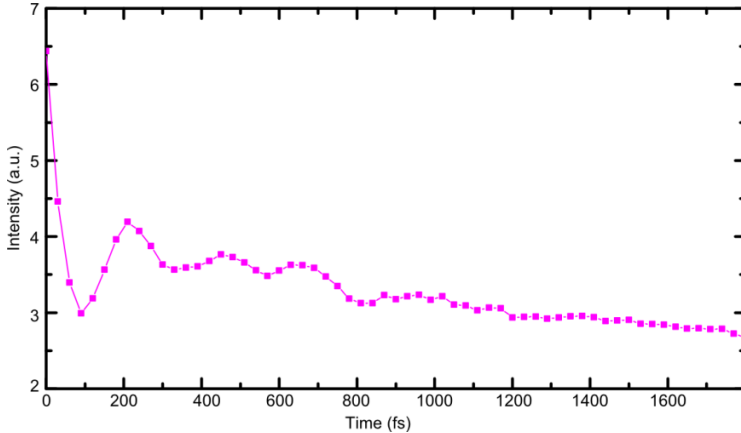


Figure S3: Coherent oscillations observed in the diagonal peak of the BChl *c* aggregate.

Experimental Setup Description

A solid state KGW amplified laser system (Pharos, Light Conversion) pumped a homemade NOPA producing 17-fs pulses centered at 12050 cm^{-1} (FWHM 1380 cm^{-1}) at 20 kHz repetition rate. Each pulse was split into four equal parts by a beamsplitter and a transmissive diffractive grating. The resulting four pulses were ordered in time using conventional optical delay lines (for the population time delays) and by inserting variable amount of fused silica in their optical paths (for the coherence time delays). One beam, serving as the local oscillator (LO), was further attenuated by an OD 3 neutral density filter, and all four pulses were focused in box-car geometry on a single spot at the sample. As the result of the sample interaction with the three laser pulses the signal pulse is emitted into the phase matching direction coinciding with the direction of LO, it is mixed with the LO and after passing through the spectrometer is detected by a CCD camera.

SUPPORTING INFORMATION

Two of the excitation pulses were modulated by optomechanical choppers operating at different frequencies. Lock-in detection on the sum and difference frequency was used to discriminate the signal against scattered light. During the experiments the time delay between the first two pulses (coherence time) was systematically scanned from -200 fs to 250 fs with 2 fs steps giving spectral resolution of about 65 cm^{-1} along the excitation axis. 50 cm^{-1} spectral resolution was achieved along the detection frequency axis, as determined by the time domain window used in the Fourier analysis.

The absorption spectrum of the sample was controlled during the measurement by monitoring the spectrum of the local oscillator passing through the sample. No changes were observed during the experiments and therefore we may conclude that the sample was stable during the measurements.